DATA REPOSITORY

Mythological background of the AFT-analyses

Apatite Fission Tracks are linear damage trails in the crystal lattice that form as the result of spontaneous nuclear fission of trace ^{238}U nuclei [*Wagner and Van den Haute, 1992*]. New tracks form at an essentially constant rate and track length, while older tracks simultaneously anneal (and ultimately are erased) at high temperatures. The annealing process causes measurable reduction in both track lengths and apparent fission track ages [e.g., *Gleadow et al., 1986; Green et al., 1989a; Green et al., 1989b*]. At temperatures higher than the total annealing temperature (T_a) between ~150 and 110 °C all fission tracks are completely annealed, resetting the fission track clock to zero. T_a depends on the kinetic characteristics of apatite and the cooling rate [*Ketcham et al., 1999*]. The partial annealing zone (PAZ) extends from the T_a down to ~60 °C, and within this temperature range tracks are partially annealed. Below ~60 °C annealing occurs at a very slow rate, therefore AFT are effectively stable [e.g., *Gleadow et al., 1986*]. The kinematic characteristics of apatite can be evaluated by measuring etch-pit figures called Dpar [*Donelick et al., 1999*]. Analytical procedures for AFT analyses and details of the sample preparation are listed with Table 1.

'*AFTSolve*' is a computer program for deriving thermal history information from apatite fission-track data. It implements a new fission-track annealing model that takes into account apatite grain composition based on either measurement of Dpar or microprobe analysis.

REFERENCE CITED

Dumitru, T.A., 1993, A New Computer-Automated Microscope Stage System for Fission-Track Analysis: Nuclear Tracks and Radiation Measurements, v. 21, no. 4, p. 575–580, doi: 10.1016/1359-0189(93)90198-I.

Dunkl, I., 2002, Trackkey: A Windows program for calculation and graphical presentation of fission track data: Computers & Geosciences, v. 28, no. 1, p. 3–12, doi: 10.1016/S0098-3004(01)00024-3.

Galbraith, R.F., 1981, On statistical models for fission-track counts: Journal of Mathematical Geology, v. 13, p. 471–478, doi: 10.1007/BF01034498.

Galbraith, R.F., and Laslett, G.M., 1993, Statistical models for mixed fission-track ages: Nuclear Tracks and Radiation Measurements, v. 21, p. 459–470, doi: 10.1016/1359-0189(93)90185-C.

Gansser, A., 1964, Geology of the Himalayas: London, Interscience Publishers, 289 p.

Green, P.F., 1981, A new look at statistics in fission-track dating: Nuclear Tracks and Radiation Measurements, v. 5, p. 77–86.
Hurford, A.J., and Green, P.F., 1983, The zeta-age calibration of fission-track dating: Isotope Geoscience, v. 1, no. 4, p. 285–317.
Watts, D.R., and Harris, N.B.W., 2005, Mapping granite and gneiss in domes along the North Himalayan antiform with ASTER SWIR band ratios: Geological Society of America Bulletin, v. 117, no. 7-8, p. 879–886, doi: 10.1130/B25592.1.

(Ref. Table 1: [Galbraith, 1981; Green, 1981; Hurford and Green, 1983; Dumitru, 1993; Galbraith and Laslett, 1993; Dunkl, 2002; Watts and Harris, 2005])

Figure DR1. Quartzitic mylonite at the base of the LPSZ hanging wall. Mylonitic stretching lineation is oriented east-west. Rocks are exposed above the village of Leo (see Fig. 2 for location).

Figure DR2. $^{40}Ar/^{39}Ar$ results from white mica and biotite in the footwall of the Leo-Pargil detachment system presented as inverse isochrons and apparent age spectra. Increments denote number of temperature steps used for the age calculation. Filled rectangles in the age spectra are those steps used to define the plateau age. Both biotite and white mica yield well-constrained plateau ages between 16 and 14 Ma. TFA = integrated total fusion age. WMPA = weighted mean plateau age. MSWD = mean square weighted deviation, an indicator of goodness of fit.

Sample number	Altitude [m]	Latitude [DM]	Longitude [DM]	Rock type	Formation	# Xls	Spontaneous		Induced		Dosimeter		Chi-sq. P (%)	Pooled Age [Ma]	±1σ	Dpar [µm]/ ±σ/ n	Uran. [ppm]	Mean tracklength [µm]/ ±σ/ n
							Rho-S	Ns	Rho-I	Ni	Rho-D	Nd						
RT01-50	2600	N 31° 48.290'	E 078° 38.538'	granite	Haimantas	25	0.422	72	29.628	5055	11.015	4721	94	3.1	0.4	2.51/ 0.17/ 100	35	
RT01-59	4670	N 31° 57.934'	E 078° 40.321'	granitic dike	Haimantas	8	2.038	120	81.616	4806	11.537	4754	96	5.6	0.7		84	
RT01-66	4950	N 31° 57.616'	E 078° 41.345'	granitic dike	Haimantas	9	2.243	178	63.017	5001	11.566	4754	1	8.0	0.8		64	
RT01-67	4160	N 31° 59.008'	E 078° 38.817'	granitic dike	Haimantas	25	1.220	266	76.360	16646	11.625	4754	71	3.6	0.3	2.33/ 0.10/ 100	81	14.31/ ±1.88/ 61
RT01-68	3770	N 31° 58.658'	E 078° 37.900'	granitic dike	Haimantas	20	0.897	251	73.712	20625	11.654	4754	52	2.8	0.3	2.34/ 0.08/ 84	75	
RT01-69	3200	N 31° 58.640'	E 078° 36.810'	granitic dike	Haimantas	23	0.524	114	57.764	12564	11.713	4754	21	2.1	0.2	2.33/ 0.10/ 92	60	
RT01-73	3150	N 32° 03.840'	E 078° 36.207'	paragneiss	Tethyan Himalaya	20	0.305	62	37.493	7614	11.742	4754	68	1.9	0.3		39	
RT02-62	4590	N31° 58.003'	E078° 40.207'	coarse paragneiss	Haimantas	30	1.802	512	67.124	19076	13.262	5413	57	6.9	0.6	2.64/ 0.14/ 100	62	13.92/ ±1.91/ 73
RT02-63	4930	N31° 21.113'	E078° 41.363'	coarse paragneiss	Haimantas	30	1.770	491	45.139	12520	13.005	5413	15	9.9	0.8	2.45/ 0.10/ 100	43	13.07/ ±2.16/ 47
RT02-70	2870	N31° 52.921'	E078° 36.046'	mylonite	Haimantas	30	0.180	40	9.969	2213	12.834	5413	100	4.5	0.8		10	
RT02-71	2980	N31° 51.078'	E078° 36.085'	mica schist	Haimantas	25	0.498	162	39.356	12804	12.748	5413	90	3.1	0.3	2.72/ 0.13/ 100	37	
RT02-72	2680	N31° 49.054'	E078° 38.139'	paragneiss	Haimantas	18	0.274	43	39.442	6191	12.663	5413	58	1.7	0.3	2.49/ 0.19/ 72	38	
RT02-73	2560	N31° 48.227'	E078° 38.519'	paragneiss	Haimantas	24	0.342	66	27.573	5328	12.123	4721	83	2.9	0.4	2.75/ 0.21/ 96	34	
RT02-75	2380	N31° 42.509'	E078° 32.212'	paragneiss	Haimantas	20	0.591	75	40.469	5137	12.044	4721	74	3.4	0.5	2.40/ 0.17/ 76	41	

Note: # Xls, number of individual grains dated;Rho-D, induced track density in external detector adjacent to dosimetry glass (x 10^6 tracks/cm^2); Nd number of tracks counted in determining Rho-D; Rho-S, spontaneous track density (x 10^6 tracks/cm^2); Ns, number of spontaneous tracks counted; Rho-I, induced track density in external detector (muscovite) (x 10^6 tracks/cm^2); Ni, number of induced tracks counted; Chi-sq. P (%), chi-sqare probability (Green, 1981; Galbraith, 1981); Age is the sample pooled fission track age (Hurford and Green, 1983); calculated using zeta calibration method (Galbraith and Laslett, 1993). Trackkey was used for calculating the counting results (Dunkl, 2002).

The following is a summary of key laboratory procedures. Samples were all analyzed by R. Thiede (zeta factor of 391 ± 27). Apatites were etched for 20 s in 5.5 N nitric acid at a temperature of 21.0 ±0.1°C. CN5 dosimetry glass was used as a neutron flux monitor. Samples were irradiated at Oregon State University TRIGA reactor. External detectors were etched in 40% HF, 21°C, 45 minutes. Tracks were counted with a Leica microscope with 100x air objective, 1.25x tube factor, 10x eyepieces, using transmitted light with supplementary reflected light as needed; external detector prints were located with kinetek computer-automated scanning stage (Dumitru, 1993).

The AFT analysis employs the external detector method following the zeta calibration approach of Hurford and Green (1983). Analytical precisions with and error of 0.2 to 0.8 Ma (±2σ) could be obtained from these young AFT ages due to the high U-content and the large number of grains counted per sample. Only grains with c axes parallel to slide plane were dated; zero-track grains were analyzed.

Table 1**:** Apatite fission track data from the Leopargil Region, see fig. 2 for location.

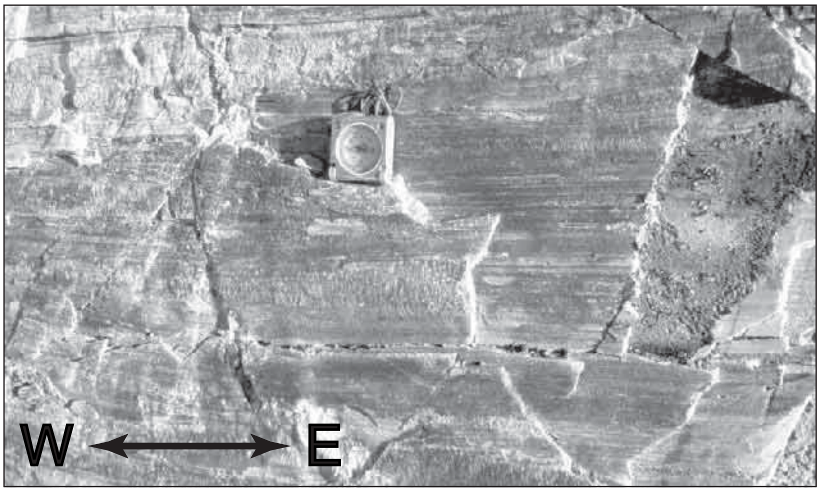

Figure DR1 data repository

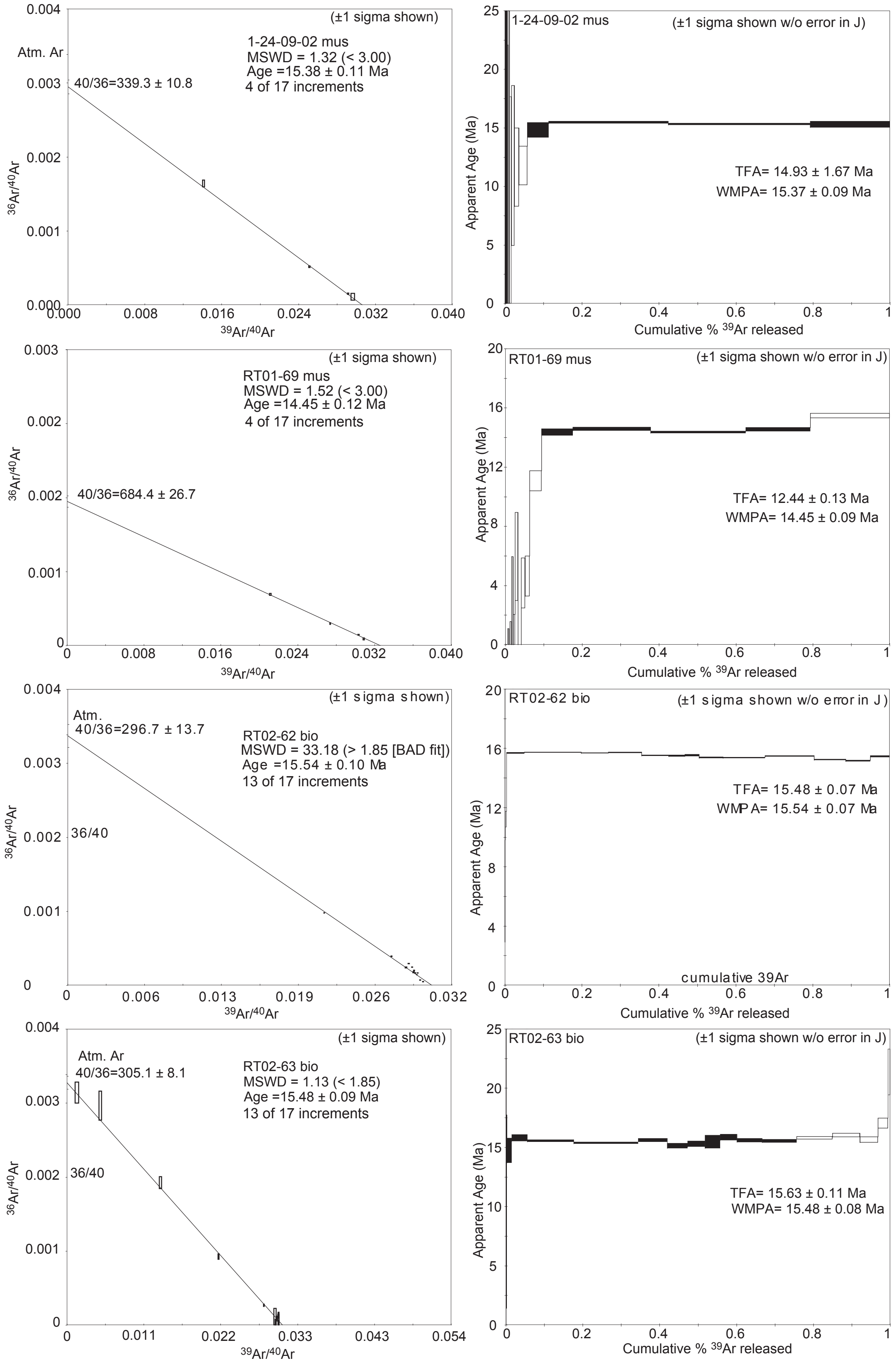

Figure DR2 data repository